Complexes between Fluorescent Cholic Acid Derivatives and Human Serum Albumin. A Photophysical Approach To Investigate the Binding Behavior

Jana Rohacova, M. Luisa Marin,* and Miguel A. Miranda*

Instituto Universitario Mixto de Tecnología Química-Departamento de Química (UPV-CSIC), Avenida de los Naranjos s/n, E-46022, Valencia, Spain

Received: November 23, 2009; Revised Manuscript Received: March 3, 2010

Interaction between bile acids and plasma proteins has attracted considerable attention over past decades. In fact, binding of bile acids to human serum albumin (HSA) determines their level in plasma, a value that can be used as a test for liver function. However, very little is known about the role that bile acids−HSA complexes play in hepatic uptake. In the present paper, we report on the utility of the singlet excited state properties of 4-nitrobenzo-2-oxa-1,3-diazole (NBD) fluorescent derivatives of cholic acid (ChA); namely, 3α-NBD-ChA, 3*β*-NBD-ChA, 3*β*-NBD-ChTau, 7α-NBD-ChA, and 7*β*-NBD-ChA to clarify key aspects of bile acids−HSA interactions that remain poorly understood. On the basis of either absorption or emission measurements, formation of NBD-ChA@HSA complexes with 1:1 stoichiometry has been proven. Enhancement of the fluorescence emission upon addition of HSA has been used for determination of the binding constants, which are in the range of 10^4 M^{-1}. Energy transfer from tryptophan to NBD-ChA occurs by a FRET mechanism; the donor−acceptor distances have been determined according to Förster's theory. The estimated values (27−30 Å) are compatible with both site I and site II occupancy and do not provide sufficient information for a safe assignment; however, fluorescence titration using warfarin (site I probe) and ibuprofen (site II probe) for displacement clearly indicates that the employed cholic acid derivatives bind to HSA at site I.

Introduction

Bile acids are steroidal tensoactives biosynthesized in the liver and which form mixed micelles with cholesterol and other lipids to enable fat digestion. For this purpose, they travel to the intestine, separate from the ingested lipids, and return to the liver for reuse in a movement known as enterohepatic circulation.[1,2] Among bile acids (Figure 1), the most abundant are cholic, deoxycholic, and chenodeoxycholic, either alone or conjugated to glycine or taurine to increase aqueous solubility at physiological pH.

On the other hand, human serum albumin (HSA) is the most abundant protein (up to 60% of the total) in blood plasma.[3] It is composed of a single polypeptide chain containing 585 amino acid residues with only one tryptophan. The three-dimensional structure is described in terms of three α-helical domains, each of them formed by two subdomains.[4,5] Interestingly, HSA plays an important role as a shuttle for a broad range of endogenous and exogenous ligands, such as fatty acids, drugs, metabolites, or bile acids. Binding of these moieties to HSA results in an increased solubility in plasma, helping delivery to the target tissues.

Experimental studies support the existence of several binding sites in HSA.[6,7] However, it is commonly accepted that there are two major structurally selective binding sites, named site I and site II, according to Sudlow's classification[8−10] (warfarin and benzodiazepine binding site, respectively). Interaction between bile acids and plasma proteins has attracted considerable attention over past decades.[11−16] In fact, binding of bile acids to HSA determines their level in plasma, a value that can be used as a test for liver function.[17,18] However, very little is known about the molecular mechanism by which the interaction takes place and also about the role that bile acid−HSA complexes play in hepatic uptake.[12]

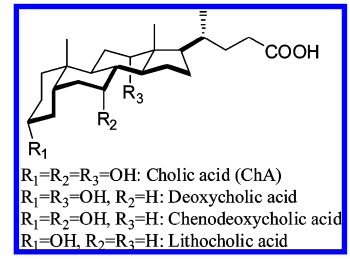

Figure 1. Structures of selected bile acids.

Several methods have been employed to gain insight into this problem, that is, equilibrium dialysis[19] or radioimmunoassay,[12] circular dichroism,[12,20] calorimetric measurements,[21] photoaffinity labeling,[22] or fluorescence microscopy.[23,24] Furthermore, in the case of lithocholic, deoxycholic, and chenodeoxycholic acids, binding to HSA has been ascribed to site II by means of difference circular dichroism or fluorescence spectroscopy using specific markers, such as dansylamide and dansylsarcosine.[19,25,26]

Excited-state properties are very sensitive to the microenvironment; therefore, they can be used to study probe distribution among the bulk solution and the different binding sites. For instance, fluorescent molecules may show strong modulation of emission properties, such as wavelength, quantum yield, or lifetime due to formation of host−guest assemblies.[27−30] Furthermore, interactions between HSA and photoactive drugs, such as carprofen and flurbiprofen, have been studied by time-resolved techniques based on the triplet excited state properties.[31−35]

We have recently reported on the use of 4-nitrobenzo-2-oxa-1,3-diazole (NBD) fluorescent derivatives at the 3α, 3*β*, 7α, and 7*β* positions of cholic acid (ChA) for uptake studies using flow cytometry.[36] The NBD fluorophore introduces only rela-

* Address correspondence to either author. Fax: (+34)963879444. E-mails: (M.A.M) mmiranda@qim.upv.es, (M.L.M) marmarin@qim.upv.es.

10.1021/jp911114n
Published on Web 03/16/2010

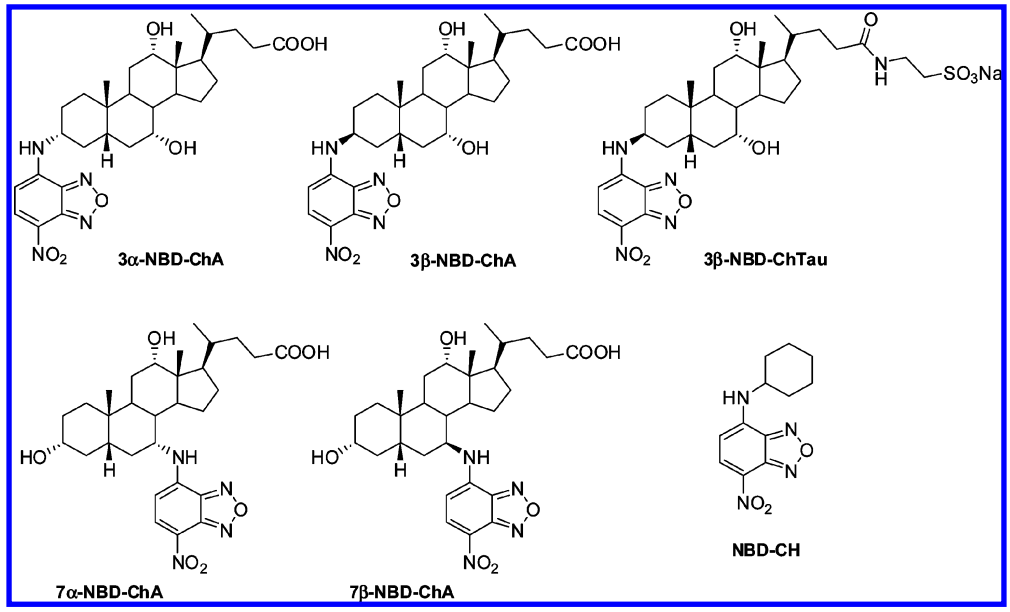

Figure 2. Structures of the compounds used for protein binding studies.

tively small changes into the molecule; therefore, it does not produce significant alterations of the physiological behavior of the parent bile acids.[37,38] As a matter of fact, the taurine conjugate of the 3β-functionalized ChA, that is, 3β-NBD-ChTau, is taken up by human sodium taurocholate cotransporting polypeptide, expressed in Chinese hamster ovary cells, with a kinetics very similar to that of nonderivatized, tritium-labeled taurocholic acid (B. Hagenbuch, private communication). Likewise, photoaffinity labeling combined with kinetic studies using isolated hepatocytes have demonstrated that 7β-NBD-ChTau is a true analog of taurocholic acid.[38] Synthetic NBD-ChA derivatives also display appropriate photophysical properties for the study of bile salt transport by fluorescent microscopy.[24,39]

In the present paper, we report on the utility of the singlet excited state properties of NBD fluorescent derivatives of cholic acid, namely, 3α-NBD-ChA, 3β-NBD-ChA, 3β-NBD-ChTau, 7α-NBD-ChA, and 7β-NBD-ChA (Figure 2), to gain deeper insight into some specific aspects of bile acid−HSA interactions. Some of these derivatives still maintain the free C-3 hydroxy group as the NBD fluorophore is attached to C-7. Conversely, in other cases, functionalization has been introduced at position C-3. In particular, the following issues require specific attention: (i) the stoichiometry of bile acid@HSA complexes; (ii) the strength of the involved interactions, with determination of the binding constants; and (iii) the safe assignment of protein binding site(s). It will be shown that 1:1 complexes are actually formed, with association constants in the range of 10^4 M^{-1}. Furthermore, binding is observed to occur at site I, as demonstrated by selective displacement probes.

Experimental Methods

Chemicals. HSA (essentially fatty acid free, 99%), (*S*)-ibuprofen, and warfarin (98%) were purchased from Sigma Aldrich and used without further purification. PBS (phosphate buffer saline) 0.01 M pH 7.4 was purchased as tablets from Sigma Aldrich and dissolved in Millipore water as indicated. The NBD derivatives were synthesized as described previously.[36,39]

Instrumentation. Absorption spectra were performed on a Cary 300 UV−vis spectrophotometer (UV0811M209, Varian). Fluorescence spectra were recorded on a LPS-220B (Photon Technology International). The absorbance of solutions at the excitation wavelength was kept below 0.1. A quartz cell of 1.00 cm optical path length was employed for all photophysical measurements. Fluorescence quantum yields were determined using fluorescein in aqueous 0.1 M NaOH ($\phi_F = 0.925$, $\lambda_{exc} =$ 470 nm) and were used as a standard.[40] The excitation wavelength was ~450 nm (isoabsorptive point) and 290 nm for titration with HSA and FRET experiments, respectively.

Sample Preparation. The concentration of NBD derivatives in PBS for the fluorescence experiments was 5 μM (obtained from 5 mM DMSO stock solution in all cases except for 3β-NBD-ChTau, which was 2.5 mM in EtOH) and titrated with 0.5 mM solution of HSA in PBS containing 5 μM of the corresponding NBD derivative. For the displacement experiments, PBS solutions of NBD derivatives (5 μM) and HSA (10 μM) were treated with warfarin or ibuprofen solutions (13 mM in DMSO in both cases). For the FRET experiments, HSA concentration was kept at 20 μM in all cases except for the 3β-NBD-ChTau experiment, which was 10 μM. The NBD analogues were added from the corresponding ethanolic stock solutions until 1 equiv was reached.

Results and Discussion

2.1. Photophysical Properties in the Presence of HSA. The UV−vis absorption spectra of the six NBD derivatives in PBS 0.01 M, pH = 7.4, showed two maxima at ~350 and 490 nm (see Figure 3 and Table 1). The fluorescence spectra showed a maximum in the range 539−555 nm upon excitation at $\lambda =$ 470 nm (Table 1). As expected, in aqueous medium, absorption and emission wavelengths were red-shifted with respect to organic solvents, and emission quantum yields were significantly lower ($\phi_F \sim 0.04$) (Table 1).[36]

After establishing the photophysical properties in phosphate buffer, the behavior in the presence of HSA was studied. For this purpose, PBS solutions containing the NBD derivative (5 μM) and different concentrations of HSA (up to 100 μM) were submitted to absorption and emission measurements. The absorption spectra, in the presence of HSA, suffered a hypsochromic shift (Table 1), together with a decrease of the absorbance (Figure 3 shows two representative examples).

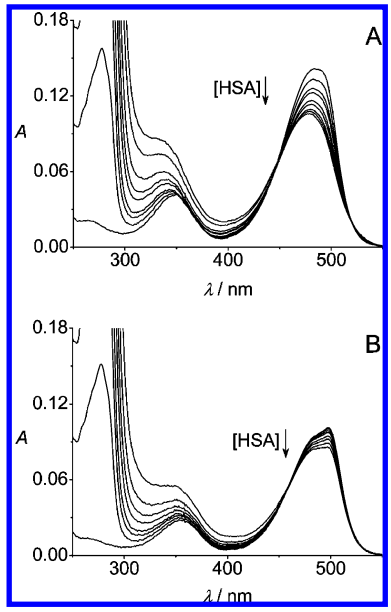

Figure 3. UV−vis spectra of (A) 3β-NBD-ChA (5 μM) and (B) 7β-NBD-ChA (5 μM) in PBS upon addition of increasing amounts of HSA (0−100 μM).

TABLE 1: Photophysical Properties of the NBD Derivatives in Aqueous Solutions (PBS 0.01 M, pH = 7.4) in the Absence and in the Presence of HSA[a]

	λ_{abs} (nm)		λ_{em} (nm)		ϕ_F			
	PBS	with HSA (20 equiv)	PBS	with HSA (20 equiv)	PBS	with HSA (20 equiv)	H_2O	ACN
3α-NBD-ChA	494	488	555	541	0.036	0.08	0.039	0.60
3β-NBD-ChA	484	479	545	521	0.043	0.16	0.040	0.55
3β-NBD-ChTau	483	476	545	519	0.042	0.22	0.044	0.66
7α-NBD-ChA	490	487	539	536	0.039	0.07	0.042	0.66
7β-NBD-ChA	498	496	547	542	0.042	0.05	0.041	0.52
NBD-CH	493	481	549	524	0.041	0.10	0.044	0.67

[a] Fluorescence quantum yields in different media are also included.

Changes in the relative absorbance were plotted against [HSA] for all the derivatives, as shown in Figure 4.

Next, the steady-state fluorescence spectra between 475 and 700 nm were recorded in the presence of increasing amounts of HSA, up to 1:20 molar ratio ($\lambda_{exc} \sim 450$ nm, isoabsorptive point). As expected from the hydrophobic nature of the protein binding sites, an enhancement in the emission intensity accompanied by a hypsochromic shift was observed under these conditions (see Figure 5 for the results obtained for 3β-NBD-ChTau and 7β-NBD-ChA as representative examples and Figure 6A for a complete set of results).

It is remarkable that not only the hydrophobicity of the HSA microenvironment seems to affect the fluorescence quantum yield but also the specific interactions between protein and fluorophore when attached to different positions of the cholic acid skeleton and with different stereochemistries. Such interactions likely involve both the space confinement provided by the binding sites and the selective NBD excited state quenching by amino acid residues located in the neighborhood. This became evident when only the hydrophobicity of the medium was progressively increased by addition of CH_3CN (see Figure 6B).

From the data of Table 1, it is clear that attachment of the NBD fluorophore at C-3β results in the highest increase in fluorescence quantum yields upon binding to HSA (up to 5-fold in the case of the 3β-NBD-ChTau), whereas in the cases of 7α-NBD-ChA and 7β-NBD-ChA, the observed effect is almost negligible (see also the end points in Figure 6A). A model compound having the NBD fluorophore attached to cyclohexylamine (NBD-CH) and lacking the steroidal skeleton was also examined for comparison; its photophysical behavior was similar to that of 3α-NBD-ChA.

The increased fluorescence intensity and the maximal blue shift are in agreement with the formation of a complex with HSA, since the excited state properties of the NBD fluorophore are strongly dependent on the nature of the microenvironment.[37,38]

2.2. Binding Behavior of NBD@HSA Complexes. ***2.2.1. Determination of Binding Constants Based on UV and Fluorescence.*** To determine the stoichiometry of the HSA complexes, absorbance changes were measured and plotted against the HSA molar fraction, keeping the total (NBD + HSA) concentration constant (see Figure 7A for a representative example). The obtained Job plots[41] indicate that a 1:1 complex is formed for all the derivatives, including the model compound (Figure 7B). Analogous experiments based on fluorescence measurements showed similar results.

When a ligand (NBD) binds reversibly to HSA to form a 1:1 complex (NBD@HSA), the change of the observed signal, S (absorbance or fluorescence response), of the reaction mixture is given by[42]

$$S = a[\text{NBD}] + b[\text{NBD@HSA}] \quad (1)$$

where S is an experimental value and a and b are proportionality constants. The equilibrium is represented by

$$[\text{NBD}] + [\text{HSA}] \underset{K_d}{\overset{K_B}{\rightleftharpoons}} [\text{NBD@HSA}] \quad (2)$$

and is governed by the equilibrium or binding constant (K_B), which is the reciprocal of the dissociation constant (K_d):

$$K_d = \frac{[\text{NBD}][\text{HSA}]}{[\text{NBD@HSA}]} \quad (3)$$

Thus, the concentration of the complex can be expressed as a function of [NBD], [HSA], and K_d, and substituting it into eq 1, the following equation is obtained,

$$S_{rel} = \frac{a[\text{NBD}]}{S_0} + \frac{b-a}{2S_0}\left([\text{NBD}] + [\text{HSA}] + K_d - \sqrt{([\text{NBD}] + [\text{HSA}] + K_d)^2 - 4[\text{NBD}][\text{HSA}]}\right) \quad (4)$$

where S_{rel} is the relative absorbance or relative fluorescence intensity (S/S_0). In practice, experiments were performed keeping [NBD] constant and varying [HSA] (in the expected order of magnitude of K_d).

Mathematical analysis of the data shown in Figure 4 or 6A in terms of eq 4, using a nonlinear least-squares algorithm, allowed determination of the binding constants (see Table 2). From these data, it can be concluded that all the NBD derivatives bind efficiently to HSA. The K_B values obtained from the absorbance and emission measurements were of the same order of magnitude; however, taking into account that the variation range in the emission measurements is higher than in the absorbance, better fittings and more reliable values were obtained in the first case.

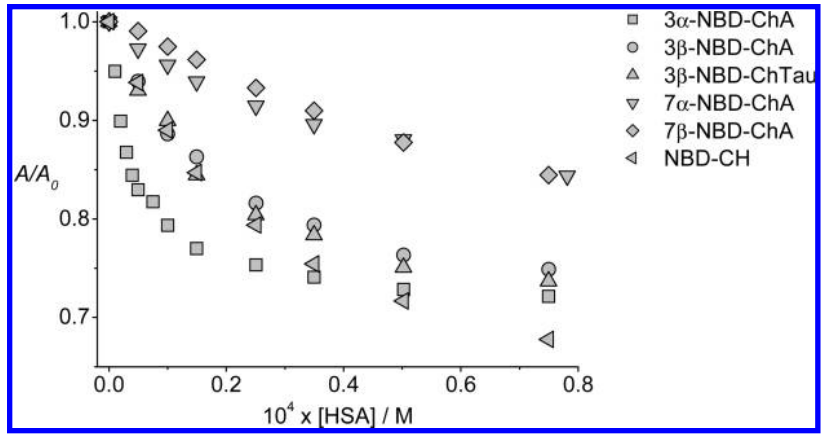

Figure 4. Changes in the relative absorbance (A/A_0) of all NBD derivatives against HSA concentration.

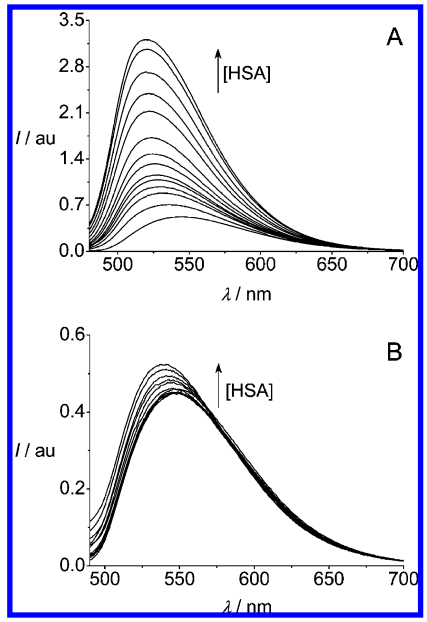

Figure 5. Emission spectra of (A) 3β-NBD-ChTau and (B) 7β-NBD-ChA (5 μM in PBS) upon addition of increasing concentrations of HSA (0−100 μM).

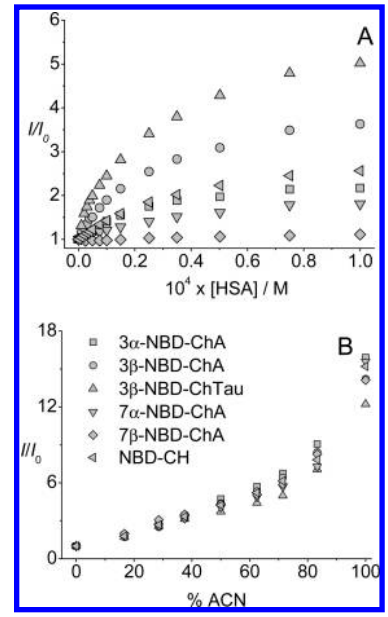

Figure 6. (A) Changes in the relative fluorescence intensity (I/I_0) of all derivatives plotted against HSA concentration. (B) Changes in the relative fluorescence intensity (I/I_0) of all derivatives in H_2O upon addition of increasing amounts of ACN.

2.2.2. Binding Assessment by Means of FRET Experiments. It is known that HSA possesses only one tryptophan residue, located at site I, and that the HSA fluorescence intensity may be sensitive to the presence of appropriate energy acceptors.[12] With this background, additional experiments were performed measuring the fluorescence spectra of HSA upon addition of increasing amounts of NBD derivatives. As shown in Figure 8 for a representative example, when a solution of HSA in PBS was excited at $\lambda = 290$ nm, the emission corresponding to tryptophan was observed. Subsequent addition of 3β-NBD-ChTau (up to 1 equiv) provoked a decrease in the Trp emission that was concomitant with an increase in the emission at ~550 nm due to 3β-NBD-ChTau. Blank experiments revealed insignificant residual emission intensity due to direct excitation of 3β-NBD-ChTau at 290 nm at the same concentration (dashed line in Figure 8). This fact, which was observed for all the analogs, reveals a very significant singlet−singlet energy transfer.

To gain a deeper insight into the operative quenching mechanisms, the Stern−Volmer equation was applied,[43]

$$I_0/I = 1 + k_q\tau_0[\mathrm{NBD}] \qquad (5)$$

where k_q is the quenching rate constant of the HSA, τ_0 is the fluorescence lifetime of HSA without quencher ($\tau = 6.38$ ns),[43] and [NBD] is the quencher concentration. In this way, k_q can be obtained from the slope of the linear plots I_0/I vs [NBD], keeping [HSA] fixed (see Figure 9 for 3β-NBD-ChA and 3β-NBD-ChTau). The calculated values were in all cases $>10^{12}$ M^{-1} s^{-1}, higher than the expected diffusion constant in biopolymers,[44] pointing to a Förster mechanism.

Hence, the quenching data can also be analyzed according to a modified Stern−Volmer equation,[45]

$$\frac{I_0}{\Delta I} = \frac{I_0}{I_0 - I} = \frac{1}{f_a K_B}\frac{1}{[\mathrm{NBD}]} + \frac{1}{f_a} \qquad (6)$$

where ΔI is the difference of fluorescence intensity in the absence and presence of the NBD derivative at a given concentration, f_a is the fraction of accessible emitting moieties, and K_B is the effective binding constant for the quenchable fluorophores. The quotient $I_0/\Delta I$ was plotted versus the reciprocal 3β-NBD-ChA and 3β-NBD-ChTau concentrations (see inset in Figure 9).

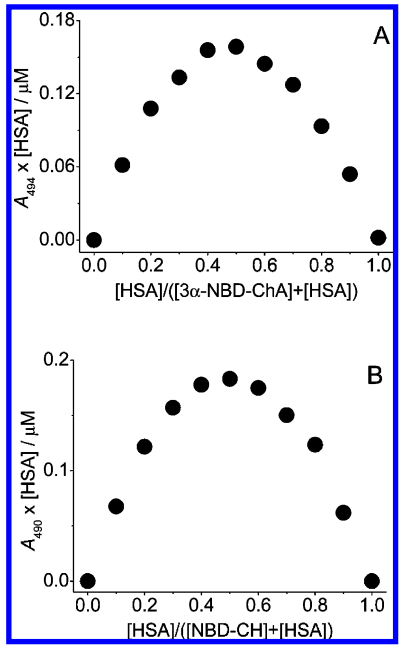

Figure 7. UV absorption Job plots for (A) 3α-NBD-ChA and (B) NBD-CH plotted against the HSA molar fraction at a total concentration ([NBD] + [HSA]) of 5 μM.

TABLE 2: Calculated Binding Constants for NBD@HSA Complexes[a]

	K_B (M^{-1}) (from UV)	K_B (M^{-1}) (from fluorescence)
3α-NBD-ChA	$(8.45 \pm 1.60) \times 10^4$	$(3.55 \pm 0.16) \times 10^4$
3β-NBD-ChA	$(4.56 \pm 0.61) \times 10^4$	$(3.65 \pm 0.12) \pm 10^4$
3β-NBD-ChTau	$(4.32 \pm 0.55) \times 10^4$	$(4.98 \pm 0.11) \times 10^4$
7α-NBD-ChA	$(1.81 \pm 0.45) \times 10^4$	$(2.10 \pm 0.16) \times 10^4$
7β-NBD-ChA	$(1.20 \pm 0.18) \times 10^4$	$(0.51 \pm 0.20) \pm 10^4$
NBD-CH	$(2.23 \pm 0.23) \times 10^4$	$(2.47 \pm 0.09) \times 10^4$

[a] Fittings were done according to eq 4.

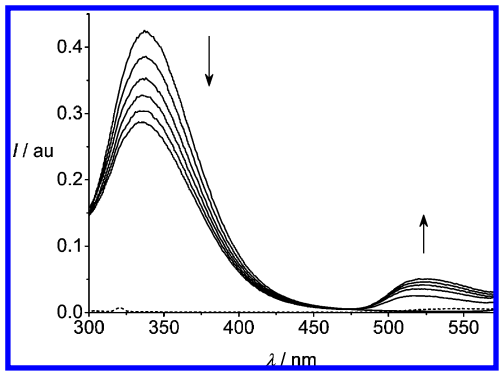

Figure 8. Emission spectra of HSA (10 μM) in PBS upon addition of increasing amounts of 3β-NBD-ChTau (up to 10 μM), λ_{exc} 290 nm. The dashed line corresponds to a blank experiment with the highest NBD concentration in the absence of HSA.

From the slope of the corresponding regression curves, the binding constant values were determined as 5.18×10^4 M^{-1} and 3.90×10^4 M^{-1}, in agreement with those obtained by using the UV absorbance and the intrinsic NBD fluorescence (see above, Table 2).

According to Förster's theory,[46] the efficiency of energy transfer (E) by a FRET mechanism (eq 7) depends on the inverse sixth-distance between donor and acceptor (r) as well

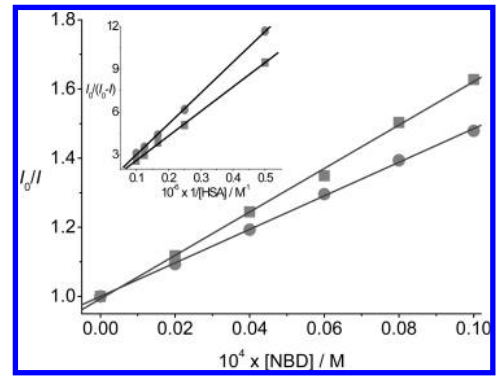

Figure 9. Stern−Volmer plot of I_0/I vs 3β-NBD-ChA (■) and 3β-NBD-ChTau (●). Inset: modified Stern−Volmer plot for the same derivatives.

as on R_0, which is defined as the critical distance at which the energy transfer is 50% (at a 1:1 donor/acceptor ratio),

$$E = \frac{R_0^6}{R_0^6 + r^6} = 1 - \frac{I}{I_0} \tag{7}$$

where I and I_0 are the fluorescence intensities of donor in the presence and in the absence of acceptor. Then, R_0 is expressed as

$$R_0 = 9.78 \times 10^3 (\kappa^2 n^{-4} \phi_D J)^{1/6} \text{ Å} \tag{8}$$

where κ^2 is the spatial orientation factor, n is the refractive index of the medium, ϕ_D is the fluorescence quantum yield of the donor, and J is the overlap integral of emission spectrum of donor and absorption spectrum of acceptor (see Figure 10 for 3β-NBD-ChTau). This term is expressed as shown in eq 9,

$$J = \frac{\int_0^\infty F(\lambda)\, \varepsilon(\lambda)\, \lambda^4\, d\lambda}{\int_0^\infty F(\lambda)\, d\lambda} \tag{9}$$

where $F(\lambda)$ is the normalized donor emission spectrum in the range from λ to $\lambda + \Delta\lambda$, and $\varepsilon(\lambda)$ is the molar absorption coefficient of the acceptor at λ.

For the NBD derivatives, calculated J values were in the range $5-9 \times 10^{-15}$ M^{-1} cm^3. Moreover, κ^2 was equal to 0.67[47] for an isotropic distribution of orientations of donor and acceptor transition dipoles, n was assumed to be 1.333 for 0.01 M PBS

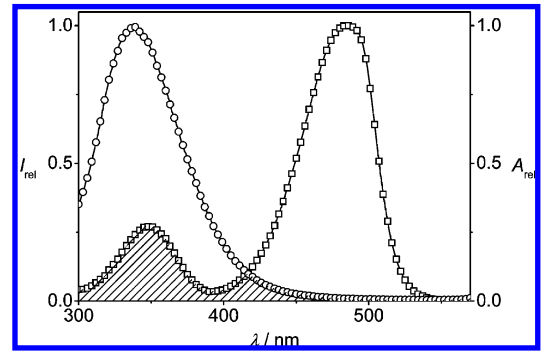

Figure 10. Spectral overlap of HSA fluorescence (○) and 3β-NBD-ChTau absorption (□) in PBS (both are normalized).

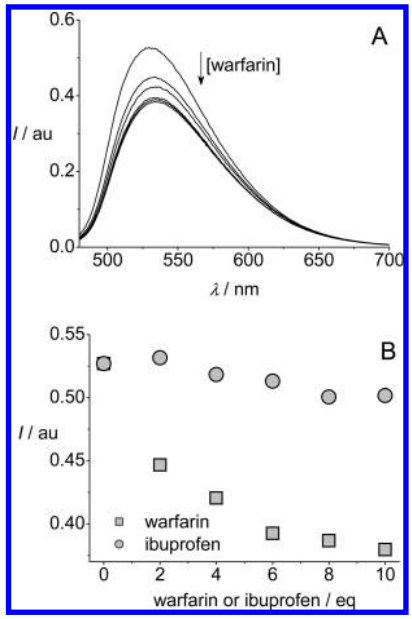

Figure 11. (A) Emission spectra of 3β-NBD-ChA (5 μM) and HSA (10 μM) in the presence of increasing concentrations of warfarin (λ_{exc} = 445 nm) and (B) changes in the emission intensity at λ_{em} = 545 nm upon addition of increasing amounts (0−50 μM) of warfarin (■) or ibuprofen (●).

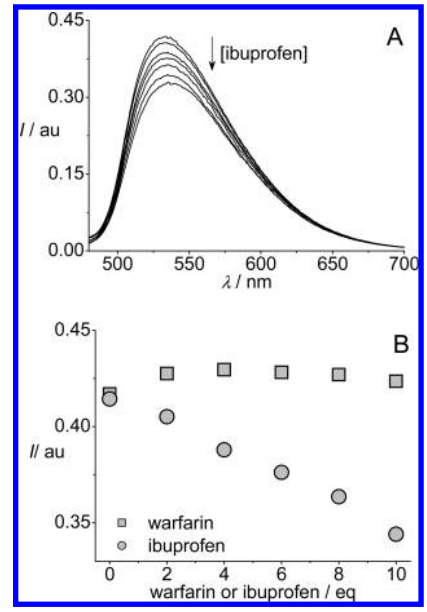

Figure 12. Emission spectra of NBD-CH (5 μM) and HSA (10 μM) in the presence of increasing concentrations of ibuprofen (λ_{exc} = 445 nm) and (B) changes in the emission intensity at λ_{em} = 545 nm upon addition of increasing amounts (0−50 μM) of warfarin (■) or ibuprofen (●).

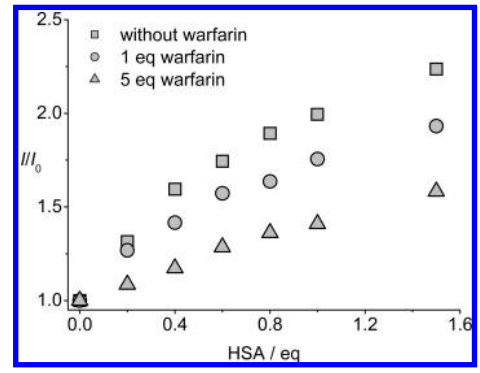

Figure 13. Emission spectra of 3β-NBDChTau (5 μM) in the presence of warfarin (0, 5, and 25 μM) with increasing concentrations of HSA (0−7.5 μM) (λ_{exc} = 445 nm).

pH = 7.4, and ϕ_D was taken as 0.15.[48] Using these parameters, the calculated R_0 values were between 23 and 25 Å, and the estimated distances (r) between tryptophan and the NBD fluorophore were 26−30 Å. These results explain the observed quenching and are compatible with the presence of NBD derivatives in either site I or site II of HSA. It has to be emphasized that r is the distance between the Trp unit and the fluorescent NBD substructure. Hence, the relatively large values found for this parameter do not apply to the distant (up to 20 Å) carboxylic acid terminus of cholic acid, which can therefore be much closer to Trp.

2.2.3. Binding Site Assignment. At this point, the formation of NBD@HSA complexes was proven, and the corresponding K_B values were calculated. The next step was to investigate the nature of the HSA binding site by displacement experiments using typical site I (warfarin) and site II (ibuprofen) probes. In this context, it is known that the binding constants to HSA are 3.0×10^5 M^{-1} for warfarin and 4.7×10^5 M^{-1} for ibuprofen.[42] Thus, aqueous solutions of NBDs (5 μM) plus 2 equiv of HSA were titrated with increasing concentrations of the displacement probes (up to 50 μM), and the fluorescence intensity was monitored. A significant decrease in the emission intensity versus warfarin concentration was observed, whereas only minor changes were noticed upon addition of ibuprofen (see Figure 11). The same behavior was observed for the other analogs, except for NBD-CH, which was displaced by ibuprofen and resulted in insensitivity to warfarin (Figure 12). This is a clear indication that the steroidal skeleton rather than the NBD moiety determines the binding site to HSA.

Further support for binding of the NBD derivatives of ChA to site I of HSA was obtained by competitive experiments, where formation of NBD@HSA was tried in the presence of warfarin. As expected, the fluorescence enhancement was less remarkable under these conditions (see Figure 13).

Conclusions

In summary, five NBD derivatives of cholic acid plus a model compound containing the fluorophore and lacking the steroidal skeleton have been used to rationalize the interactions between bile acids and HSA using emission from the single excited state as a reporting tool. Using either absorption or emission measurements, formation of NBD-ChA@HSA complexes with 1:1 stoichiometry has been proven. Enhancement of the fluorescence emission upon addition of HSA allowed determination of the binding constants in the range of 10^4 M^{-1}. Energy transfer from tryptophan to NBD occurs by a FRET mechanism; the donor−acceptor distances have been determined according to Föster's theory. The estimated values (27−30 Å) are compatible with both site I and site II occupancy. Finally, fluorescence titration using warfarin (site I probe) and ibuprofen (site II probe) for displacement clearly indicates that the employed cholic acid derivatives bind to HSA at site I.

Acknowledgment. Financial support from the CSIC (fellowship I3P-2005), the Spanish Government (RIRAAF RETICS), and the Generalitat Valenciana (Prometeo Program) is gratefully acknowledged.

References and Notes

(1) Hofmann, A. F. *Handbook of Physiology. Section 6: Alimentary Canal*; American Physiological Society: Washington, DC, 1968; Vol. 5, Bile Digestion: Ruminal Physiology.

(2) Fromm, H.; Hofmann, A. F. *Advances in Internal Medicine and Pediatrics*; Springer: New York, 1975; Vol. 37.
(3) Peters, T. *All about Albumin; Biochemistry, Genetics and Medical Applications*; Academic Press: New York, 1995.
(4) He, X. M.; Carter, D. C. *Nature* **1992**, *358*, 209.
(5) Carter, D. C.; Ho, J. X. *Adv. Protein Chem.* **1994**, *45*, 153.
(6) Petitpas, I.; Bhattacharya, A. A.; Twine, S.; East, M.; Curry, S. *J. Biol. Chem.* **2001**, *276*, 22804.
(7) Zunszain, P. A.; Ghuman, J.; Komatsu, T.; Tsuchida, E.; Curry, S. *BMC Struct. Biol.* **2003**, *3*, 1.
(8) Sudlow, G.; Birkett, D. J.; Wade, D. N. *Mol. Pharmacol.* **1975**, *11*, 824.
(9) Sudlow, G.; Birkett, D. J.; Wade, D. N. *Mol. Pharmacol.* **1976**, *12*, 1052.
(10) Fehske, K. J.; Muller, W. E.; Schlafer, U.; Wollert, U. *Prog. Drug Protein Binding, Proc. Lect. Symp.* **1981**, 5.
(11) Rudman, D.; Kendall, F. E. *J. Clin. Invest.* **1957**, *36*, 538.
(12) Roda, A.; Cappelleri, G.; Aldini, R.; Roda, E.; Barbara, L. *J. Lipid Res.* **1982**, *23*, 490.
(13) Salvioli, G.; Lugli, R.; Pradelli, J. M.; Gigliotti, G. *FEBS Lett.* **1985**, *187*, 272.
(14) Ceryak, S.; Bouscarel, B.; Fromm, H. *J. Lipid Res.* **1993**, *34*, 1661.
(15) Burke, C. S.; Panveliwalla, D.; Tabaqchali, S. *Clin. Chim. Acta* **1971**, *32*, 207.
(16) Kakis, G.; Yousef, I. M.; Fischer, M. M. *Gastroenterology* **1977**, *72*, 1178.
(17) Korman, M. G.; Hofmann, A. F.; Summerskill, W. H. J. *N. Engl. J. Med.* **1974**, *290*, 1399.
(18) Barbara, L. *Ital. J. Gastroenterol.* **1978**, *10*, 8.
(19) Takikawa, H.; Sekiya, Y.; Yamanaka, M.; Sugiyama, Y. *Biochim. Biophys. Acta* **1995**, *1244*, 277.
(20) Bertucci, C.; Domenice, E.; Salvadori, P. In *The Impact of Stereochemistry on Drug Development and Use*; Aboul-Enein, H. Y., Wainer, I. W., Eds.; John Wiley & Sons: New York, 1997.
(21) Farruggia, B.; Pico, G. A. *Biochim. Biophys. Acta* **1999**, *1429*, 299.
(22) Kramer, W.; Kurz, G. *J. Lipid Res.* **1983**, *24*, 910.
(23) Buscher, H.-P.; Gerok, W.; Kurz, G.; Schneider S. In *Enterohepatic Circulation of Bile Acids and Sterol Metabolism*; Paumgartner, G., Stiehl, A., Gerok, W., Eds.; MTP-Press: Lancaster, England, 1985.
(24) Schramm, U.; Dietrich, A.; Schneider, S.; Buscher, H.-P.; Gerok, W.; Kurz, G. *J. Lipid Res.* **1991**, *32*, 1769.
(25) Bertucci, C. *Chirality* **2001**, *13*, 372.
(26) Farruggia, B.; Garcia, F.; Pico, G. *Biochim. Biophys. Acta* **1995**, *1252*, 59.
(27) Corma, A.; Garcia, H. *Chem. Commun.* **2004**, 1443.
(28) Arunkumar, E.; Forbes, C. C.; Smith, B. D. *Eur. J. Org. Chem.* **2005**, 4051.
(29) Mohanty, J.; Nau, W. M. *Angew. Chem., Int. Ed.* **2005**, *44*, 3750.
(30) Mohanty, J.; Pal, H.; Ray, A. K.; Kumar, S.; Nau, W. M. *ChemPhysChem* **2007**, *8*, 54.
(31) Lhiaubet-Vallet, V.; Sarabia, Z.; Bosca, F.; Miranda, M. A. *J. Am. Chem. Soc.* **2004**, *126*, 9538.
(32) Lhiaubet-Vallet, V.; Bosca, F.; Miranda, M. A. *J. Phys. Chem. B* **2007**, *111*, 423.
(33) Vaya, I.; Bueno, C. J.; Jimenez, M. C.; Miranda, M. A. *ChemMedChem* **2006**, *1*, 1015.
(34) Jimenez, M. C.; Miranda, M. A.; Vaya, I. *J. Am. Chem. Soc.* **2005**, *127*, 10134.
(35) Vaya, I.; Bueno, C. J.; Jimenez, M. C.; Miranda, M. A. *J. Phys. Chem. B* **2008**, *112*, 2694.
(36) Rohacova, J.; Marin, M. L.; Martinez-Romero, A.; Diaz, L.; O'Connor, J. E.; Gomez-Lechon, M. J.; Donato, M. T.; Castell, J. V.; Miranda, M. A. *ChemMedChem* **2009**, *4*, 466.
(37) Craig, I. F.; Via, D. P.; Mantulin, W. W.; Pownall, H. J.; Gotto, A. M., Jr.; Smith, L. C. *J. Lipid Res.* **1981**, *22*, 687.
(38) Schramm, U.; Fricker, G.; Buscher, H.-P.; Gerok, W.; Kurz, G. *J. Lipid Res.* **1993**, *34*, 741.
(39) Schneider, S.; Schramm, U.; Schreyer, A.; Buscher, H.-P.; Gerok, W.; Kurz, G. J. *J. Lipid Res.* **1991**, *32*, 1755.
(40) Magde, D.; Wong, R.; Seybold, P. G. *Photochem. Photobiol.* **2002**, *75*, 327.
(41) Huang, C. Y. *Methods Enzymol.* **1982**, *87*, 509.
(42) Epps, D. E.; Raub, T. J.; Kezdy, F. J. *Anal. Biochem.* **1995**, *227*, 342.
(43) Abou-Zied, O. K.; Al-Shihi, O. I. K. *J. Am. Chem. Soc.* **2008**, *130*, 10793.
(44) Ware, W. R. *J. Phys. Chem.* **1962**, *66*, 455.
(45) Lehrer, S. S. *Biochemistry* **1971**, *10*, 3254.
(46) Förster T. *Modern Quantum Chemistry*; Academic Press: New York, 1996; Vol. 3.
(47) Förster, T. *Discuss. Faraday Soc.* **1959**, *27*, 7.
(48) Cui, F. L.; Fan, J.; Ma, D.-L.; Liu, M.-C.; Chen, X.-G.; Hu, Z.-D. *Anal. Lett.* **2003**, *36*, 2151.

JP911114N